# The exocyst subunit Sec3 is regulated by a protein quality control pathway

Received for publication, April 5, 2017, and in revised form, July 19, 2017 Published, Papers in Press, August 1, 2017, DOI 10.1074/jbc.M117.789867

**Caroline Kampmeyer[‡], Antonina Karakostova[‡], Signe M. Schenstrøm[‡], Amanda B. Abildgaard[‡], Anne-Marie Lauridsen[‡], Isabelle Jourdain[§1], and Rasmus Hartmann-Petersen[‡2]**

*From the [‡]Linderstrøm-Lang Center, Department of Biology, University of Copenhagen, Ole Maaløes Vej 5, 2200 Copenhagen N, Denmark and the [§]College of Life and Environmental Sciences, University of Exeter, Geoffrey Pope Building, Stocker Road, Exeter EX4 4QD, United Kingdom*

Edited by George N. DeMartino

**Exocytosis involves fusion of secretory vesicles with the plasma membrane, thereby delivering membrane proteins to the cell surface and releasing material into the extracellular space. The tethering of the secretory vesicles before membrane fusion is mediated by the exocyst, an essential phylogenetically conserved octameric protein complex. Exocyst biogenesis is regulated by several processes, but the mechanisms by which the exocyst is degraded are unknown. Here, to unravel the components of the exocyst degradation pathway, we screened for extragenic suppressors of a temperature-sensitive fission yeast strain mutated in the exocyst subunit Sec3 (*sec3-913*). One of the suppressing DNAs encoded a truncated dominant-negative variant of the 26S proteasome subunit, Rpt2, indicating that exocyst degradation is controlled by the ubiquitin-proteasome system. The temperature-dependent growth defect of the *sec3-913* strain was gene dosage-dependent and suppressed by blocking the proteasome, Hsp70-type molecular chaperones, the Pib1 E3 ubiquitin-protein ligase, and the deubiquitylating enzyme Ubp3. Moreover, defects in cell septation, exocytosis, and endocytosis in *sec3* mutant strains were similarly alleviated by mutation of components in this pathway. We also found that, particularly under stress conditions, wild-type Sec3 degradation is regulated by Pib1 and the 26S proteasome. In conclusion, our results suggest that a cytosolic protein quality control pathway monitors folding and proteasome-dependent turnover of an exocyst subunit and, thereby, controls exocytosis in fission yeast.**

During exocytosis, secretory vesicles fuse with the plasma membrane, thereby delivering membrane proteins to the cell surface and releasing material into the extracellular space. Importantly, exocytosis also provides lipids for membrane extension, which is required for growth, cell polarity, and division and is therefore critical for cell function and tissue development. In yeasts, exocytosis of hydrolytic enzymes is necessary to dissolve the cell wall (septum) between two daughter cells to complete cytokinesis (1). In general, cargoes derived from organelles are transported by motor proteins along cytoskeletal tracks toward specific areas of the plasma membrane. The initial contact between the secretory vesicles and the target membrane is mediated by tethering factors that are thought to bridge SNARE complexes on opposing membranes to allow vesicle docking and fusion with the plasma membrane (2, 3). The tethering of the secretory vesicles prior to docking and fusion with the plasma membrane is mediated by the exocyst, a phylogenetically conserved and stable octameric protein complex (4, 5). The two exocyst members Sec3 and Exo70 interact with phosphatidylinositol 4,5-bisphosphate at the plasma membrane and assemble the rest of the exocyst complex, which is trafficked to the cell surface on vesicles in an actin-dependent manner (6–10). The importance of the exocyst complex is exemplified by the fact that it is linked to a number of developmental and infectious diseases in animals, plants, and fungi (4). In simple organisms, such as the fission yeast *Schizosaccharomyces pombe*, most exocyst subunits are essential for viability, and conditional exocyst mutants display reduced secretion of hydrolytic enzymes, incomplete cytokinesis, and retarded cell growth (11–14). Not surprisingly, given its pivotal role, the function, localization, and assembly of the exocyst are modulated by posttranslational modifications, interaction with molecular switches such as GTPases, or alternative splicing (15, 16). There is, however, no information about the mechanisms by which the degradation of the exocyst occurs.

As a result of stress conditions or mutations, proteins may lose their native conformation and misfold. Because misfolded proteins tend to form toxic aggregates with other cell proteins, the accumulation of misfolded proteins represents a considerable danger to cells. To cope with such harmful protein variants, cells have evolved efficient protein quality control (PQC)[3] mechanisms that function to clear the cell of misfolded proteins (17–19). Typically, these rely on molecular chaperones that

This work was supported by the Lundbeck Foundation (to R. H. P.), the Danish Cancer Society (to R. H. P.), the Novo Nordisk Foundation (to R. H. P.), the A. P. Møller Foundation (to R. H. P.), the Aase and Ejnar Danielsens Foundation (to R. H. P.), the Danish Rheumatism Association (to R. H. P.), and the Danish Council for Independent Research (Natural Sciences) (to R. H. P.). The authors declare that they have no conflicts of interest with the contents of this article.

This article contains supplemental Fig. S1 and Table S1.

[1] To whom correspondence may be addressed. Tel.: 44-1392-722713; E-mail: i.jourdain@exeter.ac.uk.

[2] To whom correspondence may be addressed. Tel.: 45-35321718; E-mail: rhpetersen@bio.ku.dk.

[3] The abbreviations used are: PQC, protein quality control; UPS, ubiquitin-proteasome system; BZ, bortezomib; CHX, cycloheximide; DUB, deubiquitylating enzyme.

capture misfolded proteins and either refold them or guide them to degradation via the ubiquitin-proteasome system (UPS). How cells discern misfolded from native proteins remains incompletely understood but is likely to involve recognition of exposed hydrophobic regions in misfolded proteins. A number of proteins involved in targeting the misfolded proteins for degradation have been identified, particularly in yeast cells, where mutants in UPS components were identified as extragenic suppressors of point mutants in essential genes (20, 21). These observations suggest that PQC is highly diligent and thus prone to target proteins that are only slightly structurally perturbed and still functional. Similarly, some cystic fibrosis patients carry mutations in the *CFTR* gene (22, 23) that result in a full-length protein that retains biochemical function. This protein variant fails to conduct its function not because it is inactive but because it is discarded by the protein quality control system, prompting disease.

PQC is compartmentalized in the cell, and in recent years a great deal has been learned about endoplasmic reticulum–associated degradation (24, 25) and nuclear quality control (20, 26, 27). In contrast, cytosolic quality control is less well defined, although recent studies in budding yeast have shown that misfolded cytosolic proteins are often transported to the nucleus prior to degradation (28) or targeted directly in the cytosol by the E3s Ltn1, Rsp5, and Doa10 (29–31). Here we show that degradation of the exocyst subunit Sec3 depends on the proteasome, Hsp70-type molecular chaperones, the Pib1 E3 ubiquitin-protein ligase, and the deubiquitylating enzyme Ubp3.

## Results

### *The Sec3-913 protein is a proteasome target*

The fission yeast *sec3-913* strain carries a point mutation in the *sec3* gene that renders the cell temperature-sensitive (11). To further our understanding of the exocyst, we performed a screen for extragenic suppressors of the *sec3-913* temperature-sensitive growth defect at 35 °C. One of the suppressing plasmids contained a genomic DNA fragment of chromosome II encoding the first 658 bp (219 amino acids) of the proteasome subunit Mts2/Rpt2 (Fig. 1*A*).

Because full-length Rpt2 is a 361-residue essential ATPase subunit of the 26S proteasome (32), we predicted this truncated Rpt2 version to function in a dominant-negative manner, as has been shown before (21). To test the effect of proteasome mutations further, we combined the *sec3-913* mutant with a deletion in the proteasome assembly factor *nas6*$^+$. In agreement with the *sec3-913* temperature-sensitive phenotype being suppressed by reducing proteasome activity, we observed a strong restoration of growth at the restrictive temperature in the *sec3-913nas6*Δ double mutant (Fig. 1*B*).

In budding yeast, deletion of the gene encoding the proteasome subunit Sem1 (Dss1 in fission yeast) was found to suppress various exocyst mutations (33). To test whether this was also the case for fission yeast Dss1, a *sec3-913dss1*Δ double mutant was constructed and analyzed for growth at the restrictive temperature. In *S. pombe*, deletion of the *dss1*$^+$ gene results in a temperature-sensitive growth defect (34). Unlike the situation in budding yeast, we did not observe any effect of Dss1 on the growth defect of the *sec3-913* mutant in fission yeast (Fig. 1*C*). However, because Dss1/Sem1 is also linked to non-proteasomal functions (35), including transcription and mRNA maturation, this is likely to obscure a positive genetic interaction between *dss1* and *sec3* in *S. pombe* cells. However, as a further control, we also analyzed the growth of wild-type and *sec3-913* cells on medium containing sublethal amounts of the proteasome inhibitor bortezomib (BZ). In agreement with the genetic interaction data, addition of bortezomib suppressed the growth defect in a temperature- and dose-dependent manner (Fig. 1*D*). We therefore conclude that the *sec3-913* temperature-dependent growth defect is suppressed by blocking the proteasome.

This phenotype suppression suggests that Sec3-913 is a substrate of the UPS. To test this, we followed the degradation of V5-tagged wild-type Sec3 and Sec3-913 in cultures treated with the translation inhibitor cycloheximide (CHX). Both at the permissive and restrictive temperature, the wild-type Sec3 protein appeared to be fairly stable during the experiment. In contrast, degradation of the Sec3-913 protein occurred rapidly at the permissive temperature and was even more pronounced at the restrictive temperature (Fig. 1*E*). By densitometry of Western blots, we estimated the half-life of Sec3-913 at 36 °C to be $<$2 h (Fig. 1*F*), whereas wild-type Sec3 under the same conditions displayed a half-life of ~8 h (Fig. 1*F*). The observed degradation was proteasome-dependent because addition of the proteasome inhibitor bortezomib blocked the degradation (Fig. 1, *E* and *F*). Accordingly, addition of bortezomib and deletion of *nas6* increased the steady-state level of the Sec3-913 protein (Fig. 1, *G* and *H*). Addition of bortezomib did not lead to a general stress response because we did not observe any induction of Hsp70 (Fig. 1*G*). We conclude from these experiments that the Sec3-913 protein is a target of the UPS.

### *The Sec3-913 protein is partially functional at the restrictive temperature when proteasome activity is blocked*

Our observation that the *sec3-913* temperature-sensitive growth defect is suppressed by deletion of *nas6*$^+$ or addition of bortezomib suggests that the Sec3-913 protein at least partly retains function at the restrictive temperature. To test this prediction, we generated strains in which the endogenous *sec3* promoter was replaced with the strong *nmt1* promoter, leading to enhanced synthesis of Sec3 and Sec3-913. When *sec3-913* was overexpressed, we no longer observed any temperature-sensitive growth defect (Fig. 2*A*), suggesting that Sec3-913 is functional at the restrictive temperature. Thus, the temperature-sensitive growth defect is likely a consequence of a meticulous PQC pathway, leading to an insufficient cellular quantity of the Sec3-913 protein.

In *S. pombe*, Sec3 is required for the exocytosis of hydrolytic enzymes to dissolve the septum between two daughter cells during cytokinesis but also for actin patch localization and endocytosis (11). To test whether these functions of Sec3-913 were restored when protein degradation was inhibited, we first monitored cell septation by calcofluor staining. The septation defect of the *sec3-913* strain appeared gradually upon shifting

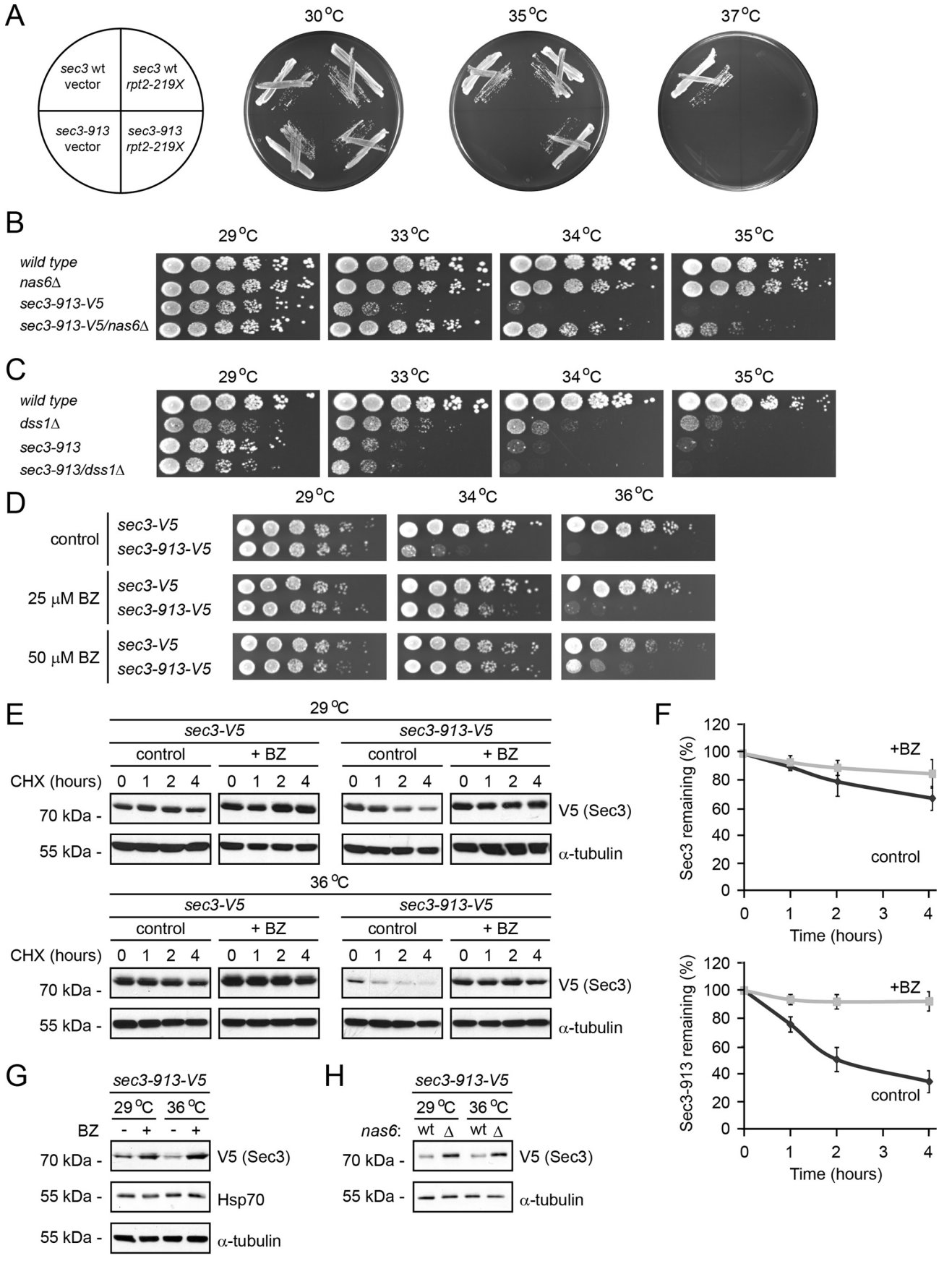
A
30 °C
35 °C
37 °C
sec3 wt vector
sec3 wt rpt2-219X
sec3-913 vector
sec3-913 rpt2-219X
B
29 °C
33 °C
34 °C
35 °C
wild type
nas6Δ
sec3-913-V5
sec3-913-V5/nas6Δ
C
29 °C
33 °C
34 °C
35 °C
wild type
dss1Δ
sec3-913
sec3-913/dss1Δ
D
29 °C
34 °C
36 °C
control
sec3-V5
sec3-913-V5
25 μM BZ
sec3-V5
sec3-913-V5
50 μM BZ
sec3-V5
sec3-913-V5
E
29 °C
sec3-V5
sec3-913-V5
control
+ BZ
control
+ BZ
CHX (hours) 0 1 2 4 0 1 2 4 0 1 2 4 0 1 2 4
70 kDa -
55 kDa -
V5 (Sec3)
α-tubulin
36 °C
sec3-V5
sec3-913-V5
control
+ BZ
control
+ BZ
CHX (hours) 0 1 2 4 0 1 2 4 0 1 2 4 0 1 2 4
70 kDa -
55 kDa -
V5 (Sec3)
α-tubulin
F
Sec3 remaining (%)
120
100
80
60
40
20
0
+BZ
control
0 1 2 3 4
Time (hours)
Sec3-913 remaining (%)
120
100
80
60
40
20
0
+BZ
control
0 1 2 3 4
Time (hours)
G
sec3-913-V5
29 °C
36 °C
BZ - + - +
70 kDa -
55 kDa -
55 kDa -
V5 (Sec3)
Hsp70
α-tubulin
H
sec3-913-V5
29 °C
36 °C
nas6: wt Δ wt Δ
70 kDa -
55 kDa -
V5 (Sec3)
α-tubulin

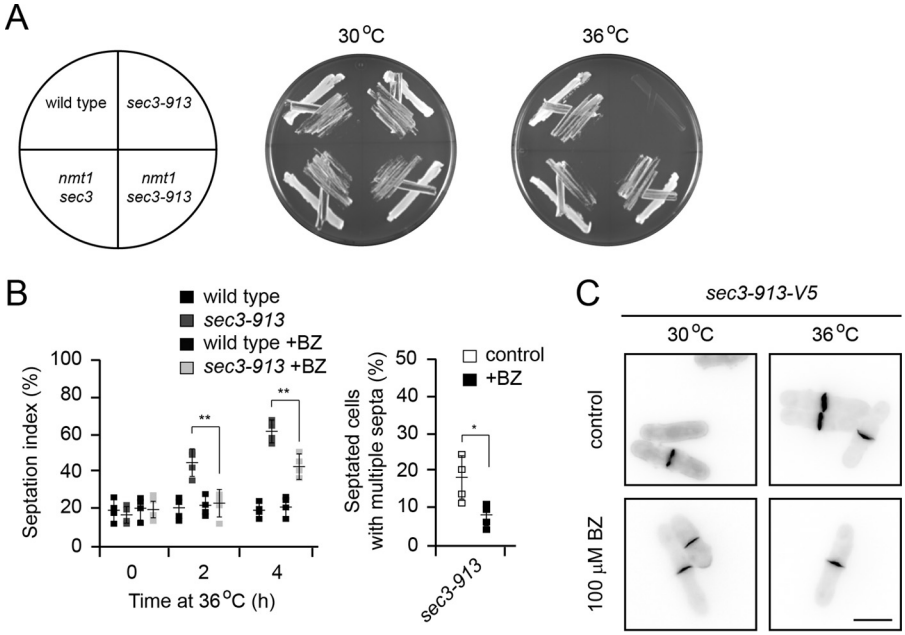


**Figure 2. Blocking the proteasome restores Sec3-913 function at the restrictive temperature.** *A*, wild-type and *sec3-913* strains, along with strains where the endogenous *sec3* promoter was replaced with the strong *nmt1* promoter, were streaked on minimal medium as indicated (*left panel*) and incubated at 30 °C and 36 °C. *B*, the percentage of septated cells (*septation index*) was determined by calcofluor staining of the indicated strains with or without added 0.2 mM BZ as a function of incubation time at 36 °C (*left panel*). The percentage of septated cells with multiple septa after 4 h at 36 °C was determined by calcofluor staining with or without added 0.2 mM BZ (*right panel*). The *error bars* indicate the standard deviation ($n = 4$). *, $p < 0.05$; **, $p < 0.01$. *C*, calcofluor staining of *sec3-913* cells at 30 °C and 36 °C with or without 0.2 mM BZ. Note that the thickness of the septa is reduced in the presence of BZ. *Scale bar* = 5 $\mu$m.

the cells to the restrictive temperature. After the cells were incubated for 4 h at 36 °C, we observed about 60% septated *sec3-913* cells, of which several displayed multiple septa. Addition of bortezomib led to a strong reduction in the number of septated and multiseptated cells (Fig. 2*B*). In addition, bortezomib treatment also reduced the thickness of the septa (Fig. 2*C*). To rule out that these results were caused by an off-target effect of bortezomib, we also analyzed septation in untreated *sec3-913nas6*Δ double mutant cells. We observed full restoration of the *sec3-913* septation defect upon deletion of *nas6* (Fig. 3*A*).

A defect in exocytosis can also be observed by transmission electron microscopy and quantified as the proportion of secretory vesicles per unit of cytoplasm. In wild-type and *nas6*Δ cells, the vesicle/cytoplasm ratio was very low, presumably because secretory vesicles efficiently fuse with the plasma membrane. In *sec3-913* cells, secretory vesicles accumulated in the cytoplasm, whereas this increase was not as extensive in the *sec3-913nas6*Δ double mutant (Fig. 3, *B* and *C*). Thus, the secretory defects observed in *sec3-913* cells are at least partially caused by the degradation of Sec3-913.

To monitor whether the reported endocytosis defect of the *sec3-913* strain (11) could be restored by deletion of *nas6*, we followed the uptake of the dye FM4-64 over time. As described previously (36), added FM4-64 first associates with the plasma membrane in zones of active growth and is then incorporated into endosomes, which later fuse with the vacuolar membranes. Clearly, FM4-64 incorporation in *sec3-913* endosomes was delayed compared with the situation in the *nas6*Δ and *sec3-913nas6*Δ double mutant (Fig. 3*D*, *arrowheads*). Hence, after 1 h, FM4-64 began to accumulate in endosomes in the *sec3-913* single mutant strain, whereas this occurred already after 30 min in the *sec3-913nas6*Δ double mutant (Fig. 3*D*). This reveals that inhibiting degradation also restores the endocytic function of the Sec3-913 protein.

### *Sec3-913 degradation depends on molecular chaperones*

Our observations so far suggest that the UPS targets the Sec3-913 protein. Because Sec3-913 is encoded by a mutant gene, is unstable, and interacts less efficiently with its binding partner Sec8 (11), we speculated that Sec3-913 is targeted for the UPS by a protein quality control mechanism, although

**Figure 1. The Sec3-913 protein is a proteasome substrate.** *A*, wild-type and *sec3-913* strains transformed with vector and the *rpt2–219X* expression construct were streaked onto minimal medium as indicated (*left panel*) and incubated at 29 °C, 35 °C, and 37 °C. *B*, growth on rich medium of wild-type, *nas6*Δ, *sec3-913*, and the double mutant was compared at the indicated temperatures. *C*, growth on rich medium of wild-type, *dss1*Δ, *sec3-913*, and the double mutant was compared at the indicated temperatures. *D*, growth on solid medium of wild-type and *sec3-913* cells was compared at the indicated temperatures in the absence (*control*) or presence of 25 or 50 $\mu$M BZ. *E*, degradation of Sec3 and Sec3-913 protein was followed in cultures at 29 °C and 36 °C, where protein synthesis was inhibited with 100 mg/ml CHX for 4 h. To some cultures 1 mM of the proteasome inhibitor BZ was also added. Tubulin served as a control for equal loading. *F*, quantification of degradation experiments as in *E*. *Top panel*, Sec3 (WT) degradation at 36 °C (*dark gray*, *filled diamonds*) and Sec3 (WT) at 36 °C with BZ (*light gray*, *filled squares*). *Bottom panel*, Sec3-913 degradation at 36 °C (*dark gray*, *filled diamonds*) and Sec3-913 at 36 °C with BZ (*light gray*, *filled squares*). The *error bars* indicate the standard error of the mean ($n = 3$). *G*, the steady-state level of Sec3-913 at 29 °C and 36 °C with or without BZ was compared by SDS-PAGE and Western blotting using antibodies to V5 (to detect Sec3-913), Hsp70 and, as a loading control, to $\alpha$-tubulin. *H*, the steady-state level of Sec3-913 at 29 °C and 36 °C in wild-type and *nas6*Δ cells was compared by SDS-PAGE and Western blotting using antibodies to V5 (to detect Sec3-913) and, as a loading control, to $\alpha$-tubulin.

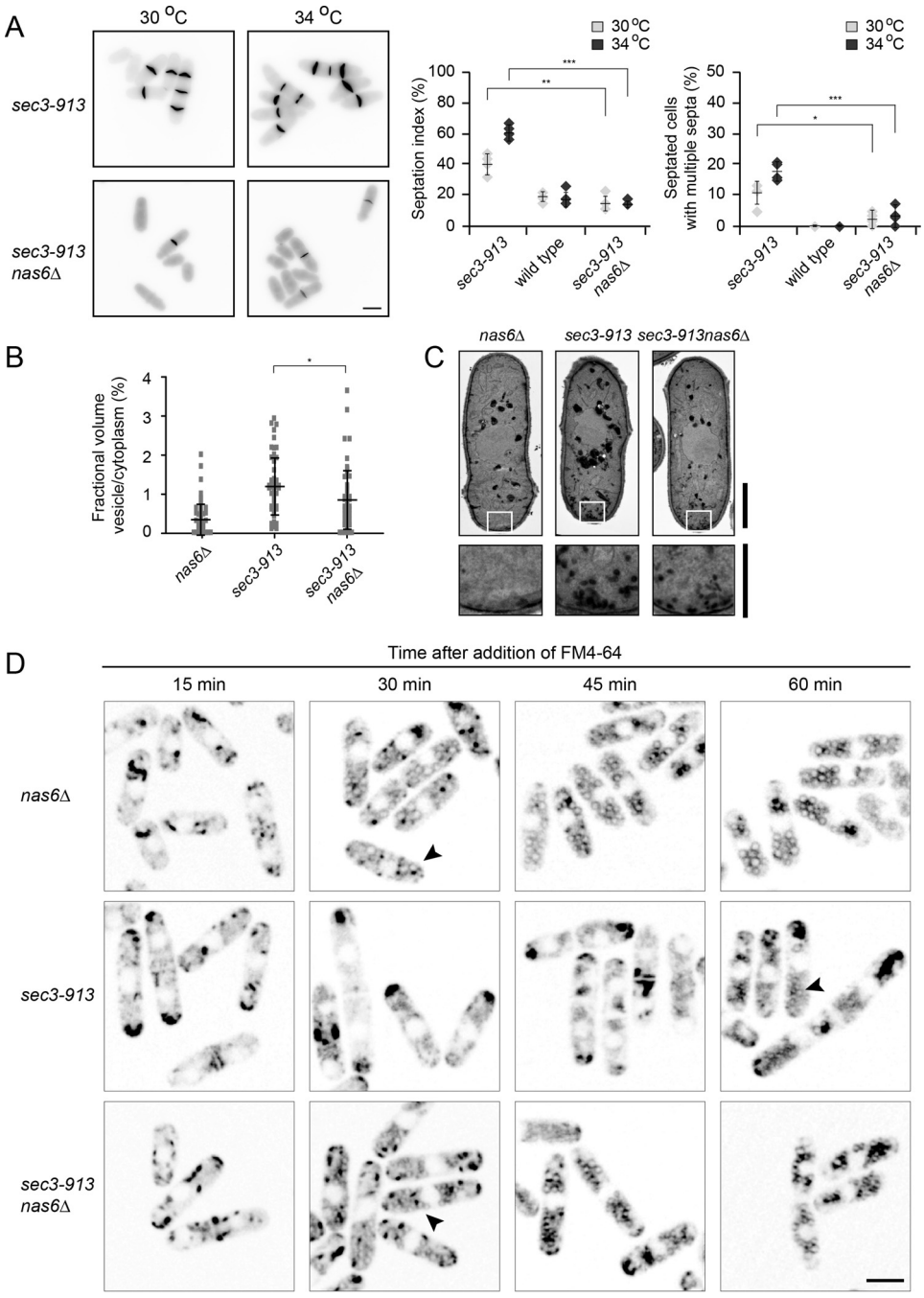


**Figure 3. Deletion of *nas6* restores Sec3-913 function in endocytosis and exocytosis.** *A*, calcofluor staining of *sec3-913* and *sec3-913nas6*Δ cells at 30 °C and 34 °C (*left panel*). The percentages of septated cells (*septation index*) and of septated cells with multiple septa were determined. The *error bars* indicate the standard deviation ($n = 4$). *, $p < 0.05$; **, $p < 0.01$; ***, $p < 0.001$. *Scale bar* = 5 $\mu$m. *B*, by electron microscopy, the fractional volume of vesicles in the cytoplasm of the indicated cells grown at 34 °C was determined. *Whiskers* mark the standard deviation ($n > 202$). The results are representative of three independent experiments. *, $p < 0.05$. *C*, transmission electron microscopy images of *nas6*Δ, *sec3-913*, and *sec3-913nas6*Δ cells at 34 °C. Higher magnifications of the *boxed areas* show fewer accumulated vesicles in *sec3-913nas6*Δ than in *sec3-913*. *Scale bars* = 2 $\mu$m for whole cells and 1 $\mu$m for the enlargement. *D*, the indicated strains were grown at 36 °C with FM4-64 dye and analyzed at regular intervals up to 1 h following addition of the dye. The accumulation of FM4-64 at the tips of *sec3-913* cells and its absence from endosomes are indicative of a defect in endocytosis. Note how this phenotype is reversed in the *sec3-913nas6*Δ double mutant (*arrowheads*). *Scale bar* = 5 $\mu$m.

Sec3-913 is still partly functional and, therefore, probably only slightly misfolded. Molecular chaperones are key players in PQC, where they catalyze folding and/or target misfolded proteins for degradation. To test whether molecular chaperones were involved in the folding or degradation of Sec3-913, we first crossed the *sec3-913* strain to different chaperone mutants to obtain double mutants. The growth of the double mutants was then compared with the single mutants at various temperatures. Deletion of the Hsp70-type chaperones *sks2*, *ssa1*, and *ssa2* led to partial suppression of the temperature-sensitive growth defect (Fig. 4*A*), indicating that these chaperones are not very active in folding Sec3-913 (because this would lead to a phenotype enhancement) but, rather, may play a role in targeting Sec3-913 for degradation. In case of *ssa2*Δ, we observed that

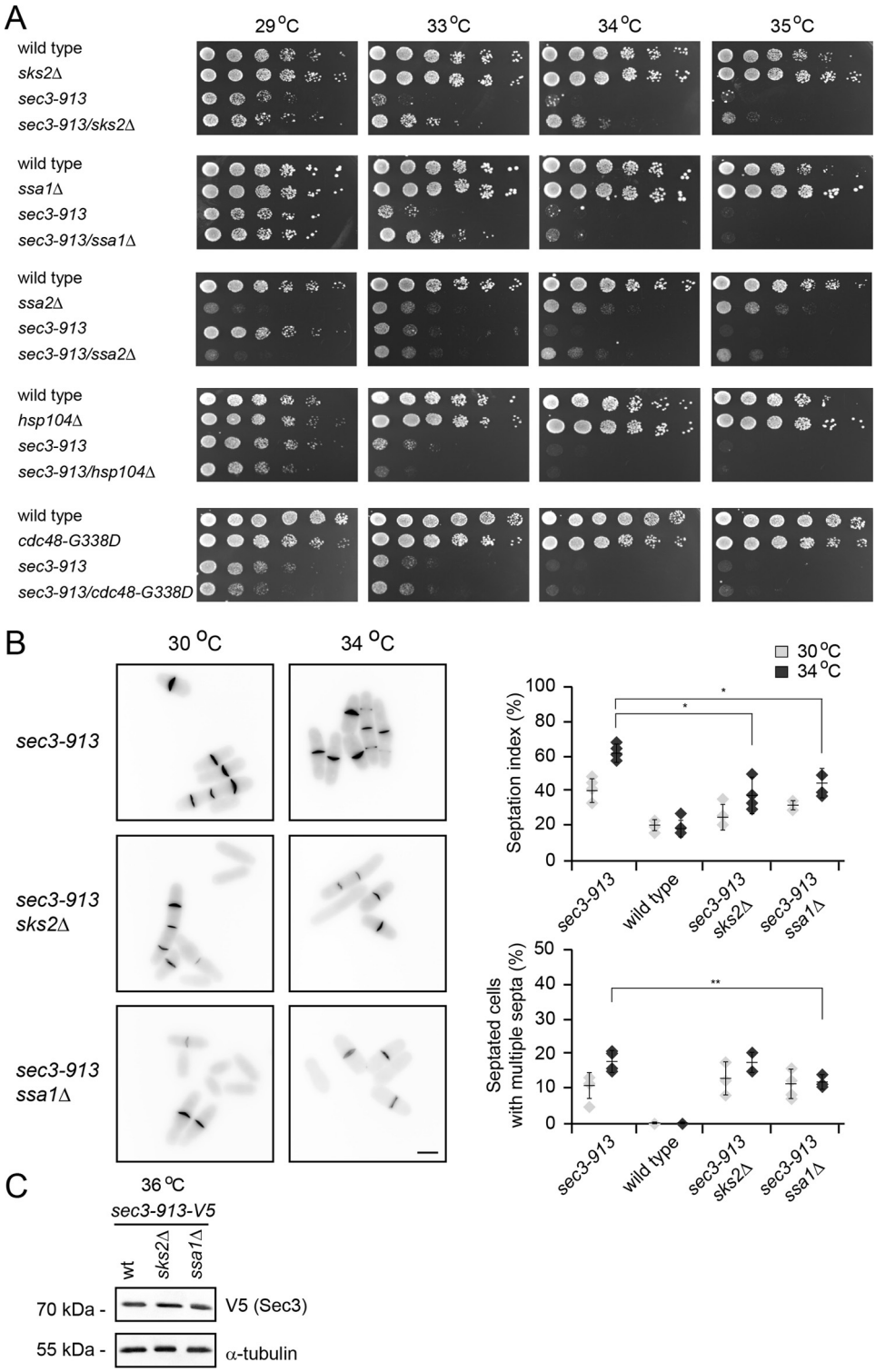


**Figure 4. Hsp70-type molecular chaperones regulate Sec3-913 levels.** *A*, growth on rich medium of the indicated mutant and double mutant strains was compared over a range of temperatures. Note that the temperature-sensitive growth defect of the *sec3-913* single mutant is suppressed in the *sec3-913sks2*Δ and *sec3-913ssa1*Δ strains. *B*, calcofluor staining of *sec3-913*, *sec3-913sks2*Δ, and *sec3-913ssa1*Δ cells at 30 °C and 34 °C (*left panel*). *Scale bar* = 5 μm. The percentage of septated cells (*septation index*) and of septated cells with multiple septa were determined. The *error bars* indicate the standard deviation ($n = 4$). *, $p < 0.05$; **, $p < 0.01$. *C*, the steady-state level of Sec3-913 at 36 °C in wild-type, *sks2*Δ, and *ssa1*Δ cells was compared by SDS-PAGE and Western blotting using antibodies to V5 (to detect Sec3-913) and, as a loading control, to α-tubulin.

the cells displayed a general growth defect that, surprisingly, appeared to be somewhat stronger at 29 °C than at higher temperatures (Fig. 4*A*). Mutation of the *cdc48* segregase did not affect the growth of the *sec3-913* strain, whereas deletion of the *hsp104* chaperone led to a slight but reproducible synthetic growth defect at 33 °C. In agreement with deletion of *sks2* and *ssa1* only partially suppressing the *sec3-913* growth defect, we only observed a modest suppression of the septation defect in

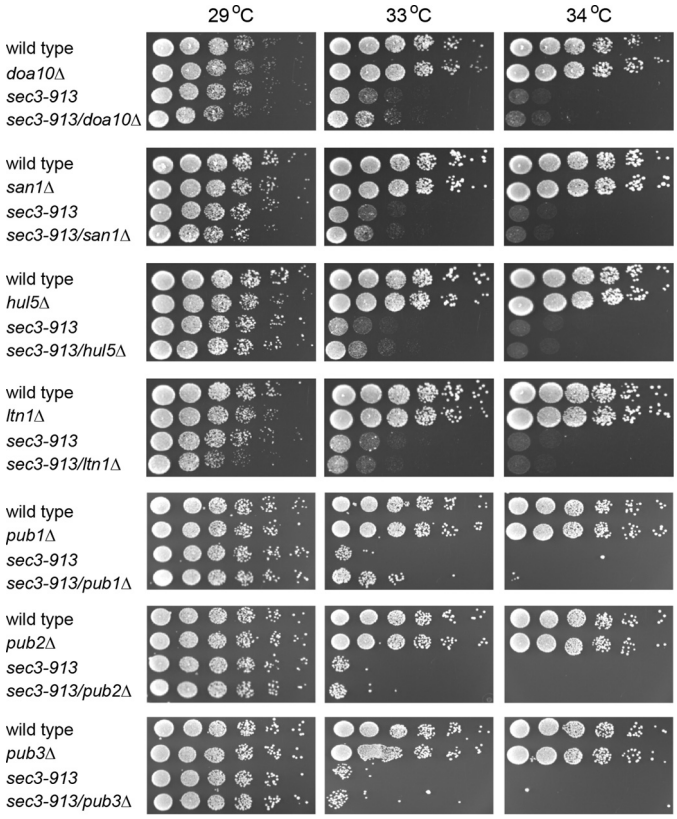


**Figure 5. Sec3-913 is not a target of typical PQC E3s but is slightly suppressed by *pub1*Δ.** The growth on rich medium of the indicated mutant and double mutant strains was compared over a range of temperatures.

the *sec3-913sks2*Δ and *sec3-913ssa1*Δ double mutants (Fig. 4*B*), and we were unable to detect any change in Sec3-913 protein levels (Fig. 4*C*).

### *The sec3-913 temperature sensitivity is partially suppressed by deletion of pub1*

To identify E3s involved in targeting Sec3-913 for degradation, we took an approach similar to the one for the molecular chaperones. In yeast, the principal nuclear quality control E3 is San1 (37), whereas Doa10, Hul5, and Ltn1 have been implicated in cytosolic quality control (29, 38–41). However, in all cases, double mutants displayed a similar growth pattern as the *sec3-913* single mutant (Fig. 5), which strongly indicates that, on their own, none of these E3s contribute significantly to Sec3-913 degradation. More recently, the budding yeast E3, Rsp5 (human NEDD4), has been connected to degradation of misfolded proteins following heat stress (30, 42). The *S. pombe* genome encodes three genes, *pub1*$^+$, *pub2*$^+$, and *pub3*$^+$, which display high similarity to *Saccharomyces cerevisiae RSP5*. When we tested these, only deletion of *pub1* led to partial rescue of the *sec3-913* temperature-sensitive growth defect (Fig. 5). This suggests that Pub1 contributes to the degradation of Sec3-913. Because double deletion mutants of *pub1*, *pub2*, and *pub3* display synthetically sick/lethal phenotypes (43, 44), we did not construct *pub* double mutants in the *sec3-913* background.

### *The Pib1 E3 ubiquitin-protein ligase targets Sec3-913 for degradation*

Because none of the typical PQC E3s appeared to target Sec3-913 for degradation, we searched the *S. pombe* database for other candidate E3s and noticed the uncharacterized SPBC36B7.05c orthologue of the budding yeast E3 Pib1 and human ZNRF2. Budding yeast Pib1 has been reported to bind phosphatidylinositol phosphate and localize to endosomal membranes (45, 46). In addition, *PIB1* expression is regulated by the heat shock transcription factor Hsf1 (47).

In agreement with Pib1 playing a role in Sec3-913 turnover, deletion of *pib1* efficiently suppressed the temperature-sensitive growth defect of the *sec3-913* strain (Fig. 6*A*). With cells on minimal medium, we observed that the temperature-sensitive growth defect of the *sec3-913* strain was less dramatic. However, overexpression of *pib1*$^+$ did not affect the growth of wild-type cells but reversed temperature-sensitive phenotype suppression of the *sec3-913pib1*Δ double mutant (Fig. 6*B*). Similar to the situation with the proteasome and chaperone mutants, deletion of *pib1* also significantly suppressed the *sec3-913* septation defect (Fig. 6*C*). In addition, the steady-state level of Sec3-913 protein was increased in a *pib1*-null background (Fig. 6*D*). Accordingly, when following the degradation of Sec3-913 in cultures treated with cycloheximide, we observed decreased degradation in *pib1*Δ cells at the restrictive temperature (Fig. 6, *E* and *F*). However, the degradation was not entirely blocked, suggesting that Pib1 is likely functionally redundant with other PQC E3s.

Finally, to test the ubiquitylation of Sec3-913, we transformed the *sec3-913* and *sec3-913pib1*Δ strains with a plasmid overproducing $His_6$-tagged ubiquitin. After blocking protein degradation with bortezomib, ubiquitin and ubiquitin-protein conjugates were isolated by precipitation using an $Ni^{2+}$ resin under denaturing conditions. Indeed, we observed that Sec3-913 was ubiquitylated and that the ubiquitylation was reduced in the *pib1*Δ background (Fig. 6*G*). In agreement with Pib1 being functionally redundant with other E3s, ubiquitylation of Sec3-913 was also still evident in the *pib1*-null strain. Also, because we did not observe any growth defect in a *pib1*Δ*pub1*Δ double mutant (supplemental Fig. S1), Pib1 and Pub1 are unlikely to generally overlap in their function.

### *Sec3-913 degradation requires deubiquitylating enzymes*

When a ubiquitylated substrate reaches the 26S proteasome, various proteasome-associated deubiquitylating enzymes (DUBs) cleave the ubiquitin chain and thus regulate degradation. For instance, the proteasome-associated DUB Ubp6 has been shown to rescue substrates from degradation by trimming ubiquitin chains (48, 49). In contrast, the proteasome-associated DUBs Ubp3 and Uch2 (UCH37 in humans) have been shown to stimulate degradation (50, 51), presumably because ubiquitylated proteins are less efficiently translocated into the proteasome lumen. In addition, the budding yeast DUBs Ubp2 and Ubp3 were recently shown to be required for degradation of misfolded proteins targeted by Rsp5 (Pub1, Pub2, and Pub3 in fission yeast) (42).

To test whether any of these DUBs regulate Sec3-913 turnover, we crossed the *sec3-913* strain to different DUB mutants to obtain double mutants. The growth of the double mutants was then compared with the single mutants at various temperatures. We did not observe any genetic interaction between *sec3-913* and *ubp2*Δ (Fig. 7*A*). Deletion of *ubp6* led to a slightly synthetic sick phenotype (Fig. 7*A*), indicating that Ubp6 may deubiquitylate Sec3-913 and thus antagonize its degradation. However, for both *uch2*Δ (the UCH37/UCHL5 orthologue in fission yeast) and *ubp3*Δ, we observed a suppression of the *sec3-*

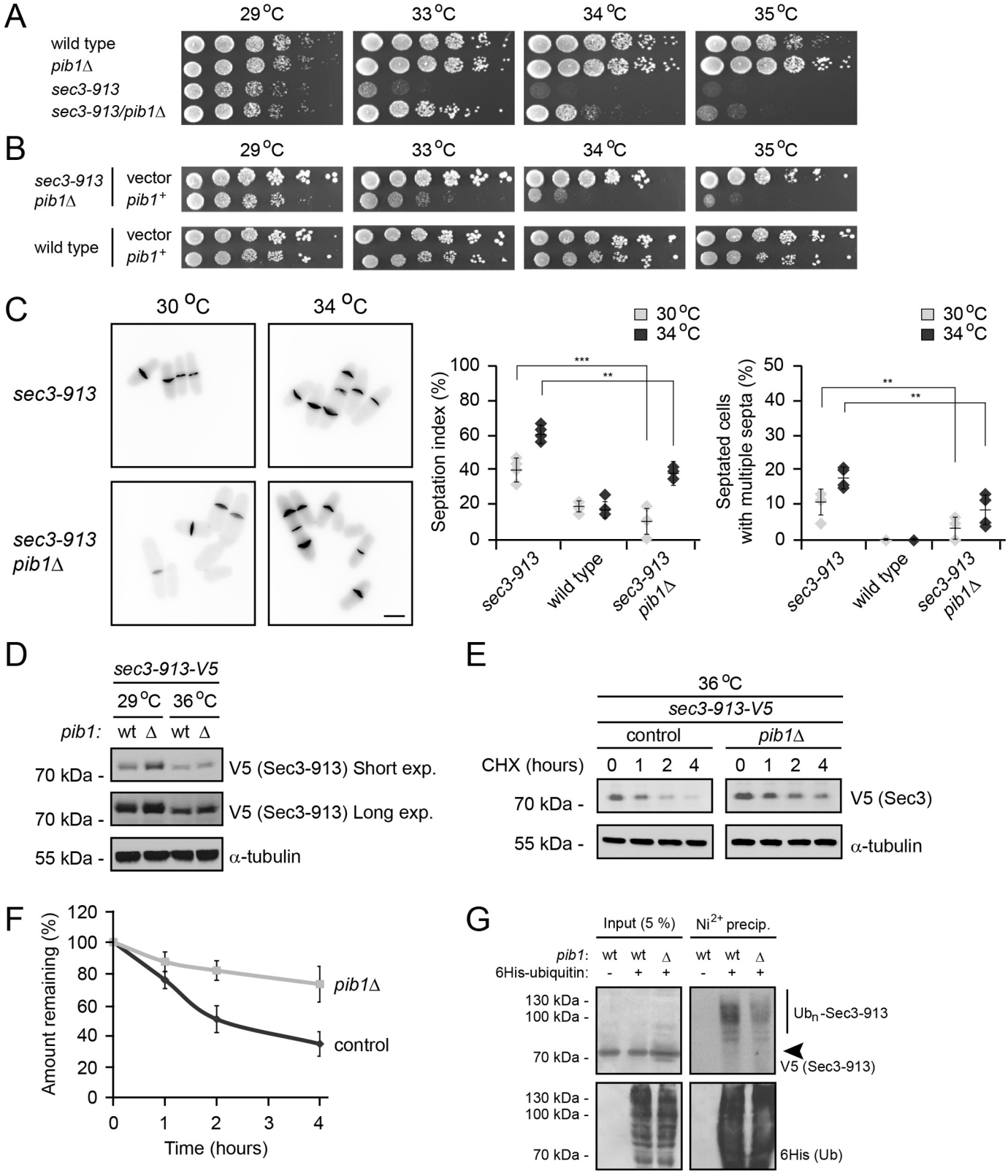

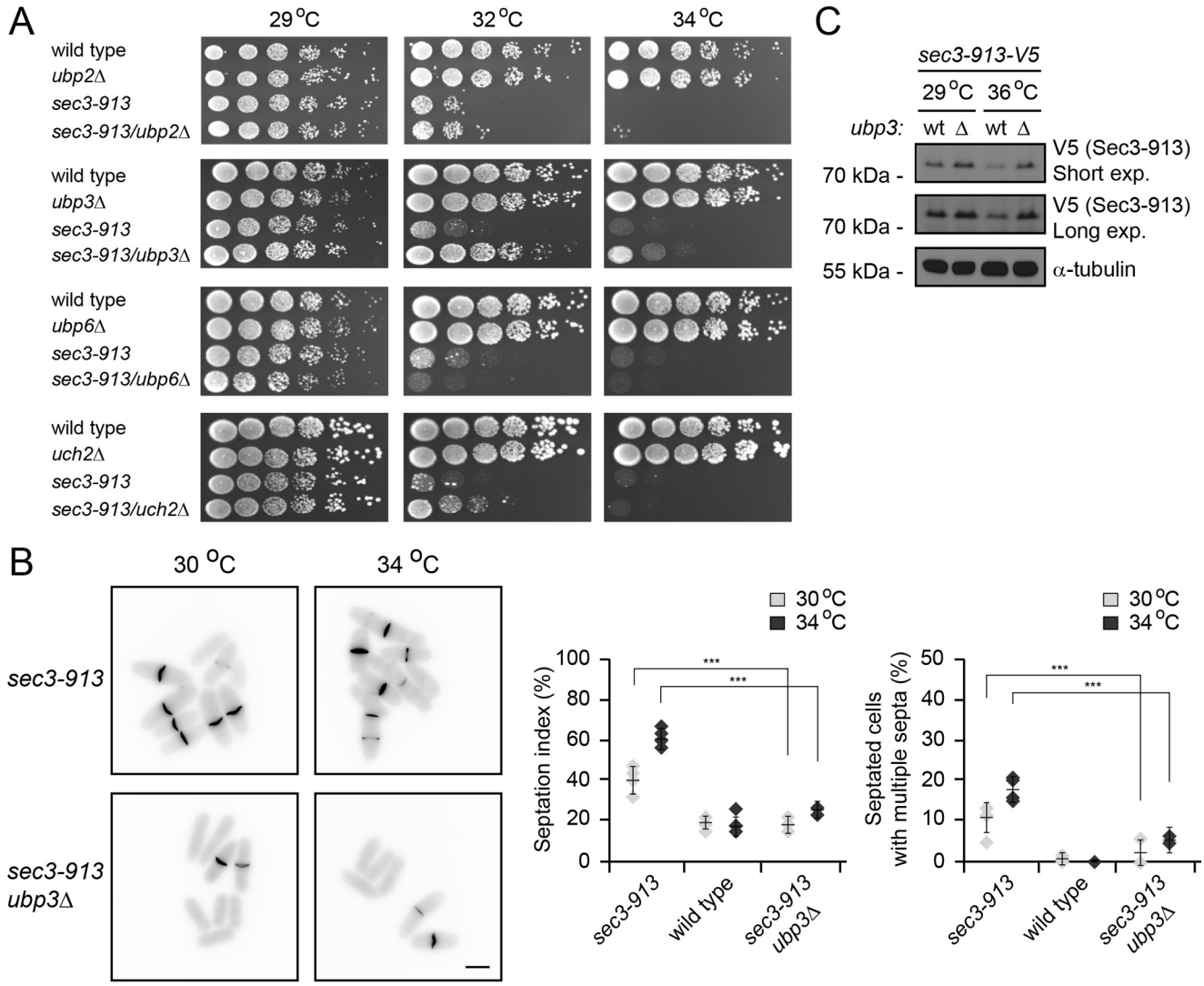


**Figure 7. Sec3-913 is a target of proteasome-associated deubiquitylating enzymes.** *A*, growth on rich medium of the indicated mutant and double mutant strains was compared over a range of temperatures. Note that the temperature-sensitive growth defect of the *sec3-913* single mutant is suppressed in *sec3-913ubp3*Δ cells and, to a lesser degree, in the *sec3-913uch2*Δ strain. *B*, calcofluor staining of *sec3-913* and *sec3-913ubp3*Δ cells at 30 °C and 34 °C (*left panel*). *Scale bar* = 5 μm. The percentages of septated cells (*septation index*) and of septated cells with multiple septa were determined. The *error bars* indicate the standard deviation ($n = 4$). ***, $p < 0.001$. *C*, the steady-state level of Sec3-913 in the indicated strains at 29 °C and 36 °C was compared by SDS-PAGE and Western blotting using antibodies to V5 (to detect Sec3-913) and, as a loading control, to α-tubulin.

*913* temperature-sensitive growth defect (Fig. 7*A*). This phenotype suppression was more pronounced for *ubp3* than for *uch2*, indicating that Ubp3 plays a more prominent role than Uch2 for regulation of Sec3-913 degradation. The septation defects of the *sec3-913* strain were also strongly alleviated in the *sec3-913ubp3*Δ double mutant (Fig. 7*B*), and, accordingly, deletion of *ubp3* led to an increase in the steady-state level of Sec3-913 protein, in particular at the restrictive temperature (Fig. 7*C*). We therefore conclude that Ubp3 and Uch2 stimulate Sec3-913 degradation. However, because we did not observe any growth defect in *ubp3*Δ*uch2*Δ double mutants (supplemental Fig. S1), either these DUBs do not

**Figure 6. The Pib1 E3 ubiquitin-protein ligase targets Sec3-913 for degradation.** *A*, growth on rich medium of wild-type, *pib1*Δ, *sec3-913*, and the double mutant was compared at the indicated temperatures. *B*, growth of the wild-type and *sec3-913pib1*Δ strains transformed with either an empty vector or a *pib1*$^+$ expression vector was compared at the indicated temperatures. To select for the plasmids, these experiments were performed on EMM2 minimal medium. Note that we found that the *sec3-913* strain was not quite as temperature-sensitive on minimal medium as on complete medium (*e.g.* in *A*). *C*, calcofluor staining of *sec3-913* and *sec3-913pib1*Δ cells at 30 °C and 34 °C (*left panel*). *Scale bar* = 5 μm. The percentages of septated cells (*septation index*) and of septated cells with multiple septa were determined. The *error bars* indicate the standard deviation ($n = 4$). **, $p < 0.01$; ***, $p < 0.001$. *D*, the steady-state level of Sec3-913 in the indicated strains was compared by SDS-PAGE and Western blotting using antibodies to V5 (to detect Sec3-913) and, as a loading control, to α-tubulin. *exp.*, exposure. *E*, the degradation of Sec3-913 protein was followed in *sec3-913* and *sec3-913pib1*Δ cultures at 36 °C, where protein synthesis was inhibited with 100 mg/ml CHX for 4 h. Tubulin served as a control for equal loading. *F*, quantification of degradation experiments as in *E*; Sec3-913 degradation at 36 °C (*dark gray*, *filled circles*) and Sec3-913 at 36 °C in the *pib1*Δ background (*light gray*, *filled squares*). The *error bars* indicate the standard error of the mean ($n = 4$). *G*, the *sec3-913-V5* strain carrying WT *pib1* or a *sec3-913-V5/pib1*Δ strain transformed with a $His_6$-tagged ubiquitin expression construct, as indicated, was treated with 1 mM bortezomib overnight, lysed, and used for precipitation (*precip.*) experiments with an $Ni^{2+}$ resin in 8 M urea. The precipitated material was analyzed by blotting with antibodies to the V5 tag on Sec3-913 or to the $His_6$ tag on ubiquitin. The *arrowhead* marks the position of non-ubiquitylated ($Ub_n$) Sec3-913.

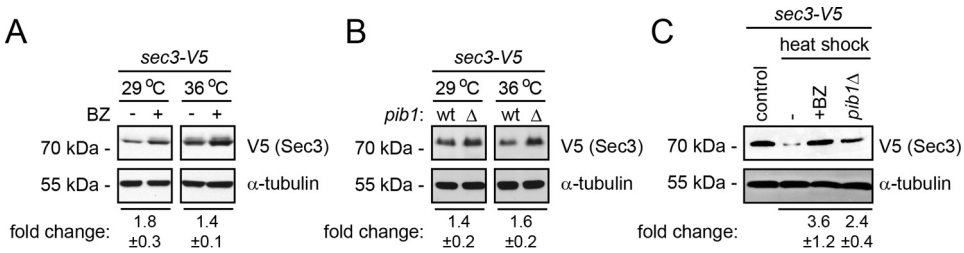


**Figure 8. Wild-type Sec3 levels are regulated by Pib1 and the proteasome.** *A*, the steady-state level of wild-type Sec3 at 29 °C and 36 °C in cultures treated with BZ for 16 h was compared by SDS-PAGE and Western blotting using antibodies to V5 (to detect Sec3) and, as a loading control, to α-tubulin. Quantifications by densitometry are given below as -fold change ± standard error of the mean ($n = 3$). *B*, the steady-state level of wild-type Sec3 at 29 °C and 36 °C in either a WT or *pib1*Δ background was compared by SDS-PAGE and Western blotting using antibodies to V5 (to detect Sec3) and, as a loading control, to α-tubulin. Quantifications by densitometry are given below as -fold change ± standard error of the mean ($n = 3$). *C*, the steady-state level of wild-type Sec3 from cells grown at 29 °C (*control*) or cells subjected to a 45-min heat shock treatment at 40 °C was compared in the presence or absence of the proteasome inhibitor BZ or in a *pib1*Δ background by SDS-PAGE and Western blotting using antibodies to V5 (to detect Sec3) and, as a loading control, to α-tubulin. Quantifications by densitometry are given below as -fold change ± standard error of the mean ($n = 3$).

generally overlap in their function or they are functionally redundant with other cellular DUBs.

### *Wild-type Sec3 is also a UPS target*

When the molecular chaperones and components of the UPS are blocked, the Sec3-913 protein appears functional at the restrictive temperature; therefore, we reasoned that, structurally, the Sec3-913 protein is most likely near native or least not highly misfolded. Accordingly, it is possible that the components involved in degradation of Sec3-913 may also, to a lesser extent, target wild-type Sec3 for degradation. In our degradation assays, the wild-type Sec3 protein appeared to be fairly stable during the experiment (Fig. 1*F*, $t_{½}$, ~8 h). The steady-state level of wild-type Sec3 was clearly increased after 16 h with bortezomib (Fig. 8*A*) and, at the restrictive temperature, also significantly increased in the *pib1*Δ strain (Fig. 8*B*), indicating that wild-type Sec3 levels are also regulated by Pib1 and the UPS. Importantly, these differences were even more pronounced after subjecting cells to a 45-min heat shock at 40 °C (Fig. 8*C*). We therefore conclude that wild-type Sec3 is likely to be regulated by a similar mechanism as we observed for Sec3-913.

## Discussion

The exocyst is an evolutionarily conserved protein complex that tethers post-Golgi vesicles, transported along cytoskeletal tracks, to the plasma membrane. As an exocyst subunit, Sec3 plays an important role in mediating interaction of the complex with the plasma membrane (6, 9). Here we show that the exocyst subunit Sec3 is regulated by a protein quality control pathway (Fig. 9). Our data suggest that this PQC pathway operates on wild-type Sec3 under stress conditions that may cause misfolding but is exacerbated in the Sec3-913 missense protein variant. This is in agreement with the previously observed depletion of Sec3 in response to heat shock and damage of the cell membrane in budding yeast (52). This also indicates that the structural stability of the Sec3-913 protein is compromised, and, accordingly, the Sec3-913 protein displays impaired interaction with the exocyst subunit Sec8 (11); as we show here, Sec3-913 is regulated by molecular chaperones. However, because exocyst function is restored upon blocking the PQC pathway, the Sec3-913 protein is probably only slightly misfolded at the restrictive temperature, which suggests that mutations that only cause subtle misfolding may still trigger rapid protein turnover. Because previous studies have shown that depletion of one exocyst subunit does not affect the level of the other subunits (5), it is unlikely that the other exocyst subunits become unstable in *sec3-913* cells at the restrictive temperature.

Early studies showed that certain missense protein variants are more rapidly degraded than wild-type proteins (53). Since then, a number of proteins involved in targeting the misfolded proteins for degradation have been identified in a manner similar to our approach, in which mutants in UPS components were identified as extragenic suppressors of point mutants in essential genes (20, 21). For instance, the nuclear PQC E3 San1 was first connected to protein quality control of the mutant proteins Sir4-9 and Cdc68-1 because loss of San1 alleviates the *sir4-9* and *cdc68-1* phenotypes (20). These observations are important because they link proteasomal substrates to E3s, which is otherwise highly complicated, in particular because of the vast number of genes encoding E3s (the human genome encodes more than 600 different E3s, whereas the fission yeast genome encodes roughly 100 different E3s). However, these genetic interactions also suggest that the PQC network is highly diligent and prone to target proteins that are only slightly structurally perturbed and still functional. This has important consequences for protein evolution (54) because mutations in proteins that allow functional innovation may slightly destabilize the structure and trigger degradation via the UPS. This severely limits the functional space available for a protein variant, and, accordingly, molecular chaperones are important for evolution because they may help destabilized mutants to fold, allowing access to new activities (55–57). However, chaperones have also been shown to actively direct their substrates for degradation (58).

This seemingly overactive PQC also has direct consequences for disease. For instance, missense variants in the mismatch repair protein MSH2 have been linked to the hereditary cancer predisposition syndrome, known as Lynch syndrome. Although several of the disease-linked *MSH2* mutations result in functional proteins with only minor folding defects, the proteins are targeted for degradation, leading to depletion of the MSH2 protein, which, in turn, triggers the disease (59, 60). As mentioned, similar observations have been made for cystic

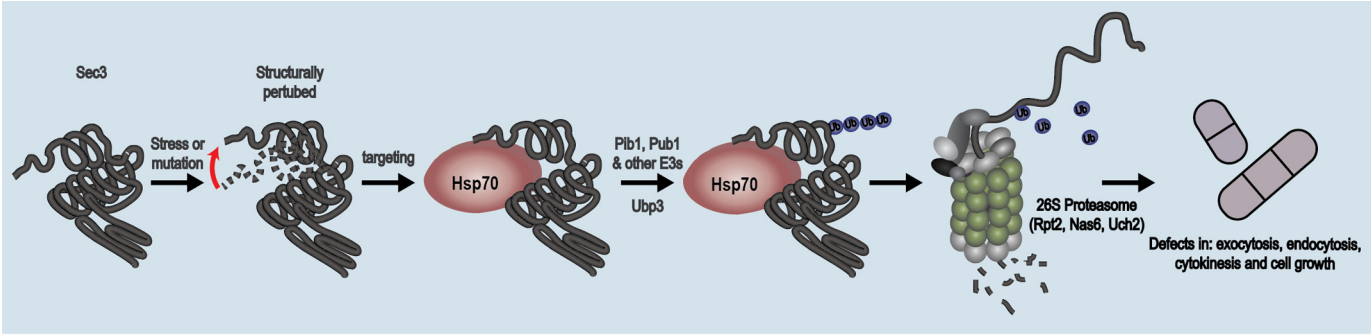


**Figure 9. Model for protein quality control of the exocyst.** The data presented here are compatible with a model in which the Sec3 protein, in response to mutations or a stress condition, becomes structurally perturbed, and molecular chaperones detect it as being misfolded. The protein is then ubiquitylated by Pib1 and other E3s, such as Pub1, and directed to the 26S proteasome. At the 26S proteasome, the protein is degraded, leading to loss of function and defects in exocytosis, endocytosis, cytokinesis, and cell growth.

fibrosis and disease-linked variants of the CFTR protein (23), suggesting that this highly sensitive PQC system may be a common etiological mechanism for disease-linked loss-of-function missense mutations.

In general, the nuclear and endoplasmic reticulum–associated degradation pathways for degradation of misfolded proteins are well characterized (20, 24, 26, 27). However, PQC in the cytosol is less well defined. Recent studies in budding yeast have shown that smaller misfolded cytosolic proteins are transported to the nucleus, where they are ubiquitylated by the E3 San1 and degraded (26, 28, 61). Other misfolded cytosolic proteins appear to be targeted during translation on the ribosome (62–64) or directly in the cytosol by the E3s Ltn1, Rps5, and Doa10 (29, 42). We found that the degradation of Sec3-913 occurred independent of San1, Ltn1, and Doa10 but relied on the membrane-associated Pib1 enzyme. However, we note that some Sec3-913 is still degraded when *pib1* is deleted, suggesting that Sec3-913 can also be targeted for degradation via other pathways. This observation is in line with studies in budding yeast that have shown that multiple E3s display overlapping substrate specificity for misfolded proteins (65). Indeed, we observed that the *sec3-913* temperature-sensitive growth defect is partially suppressed by deletion of *pub1*, suggesting that Pub1 also contributes to Sec3-913 degradation. In addition, the strong suppressing effect we observed for *ubp3*Δ and the link between Rsp5 and Ubp3, recently established in budding yeast (42), lend additional support for a role of Pub1 in Sec3-913 degradation. The fission yeast *pub1*$^+$, *pub2*$^+$, and *pub3*$^+$ genes are highly similar and unessential orthologues of the essential *RSP5* gene in *S. cerevisiae* (43). Accordingly, *pub1*$^+$, *pub2*$^+$, and *pub3*$^+$ display overlapping functions and pairwise synthetic deletion phenotypes (43, 66), indicating that they may all contribute to Sec3-913 turnover. However, because Rsp5 and the fission yeast Pub E3s have also been linked to other functions, including transcription, ribosome stability, and endocytosis (66–71), they may also indirectly contribute to the *sec3-913* phenotype.

As for how the cellular PQC system is able to discriminate between misfolded proteins and their native counterparts, this has been shown, in the case of San1, to involve direct recognition of exposed hydrophobic regions in the substrate (20). However, other PQC E3s seem to associate with molecular chaperones and ubiquitylate the chaperone-bound substrates (58). Because we found that the Hsp70-type chaperones Sks2 and Ssa1 both affect Sec3-913, Pib1 presumably operates through molecular chaperones. Sec3-913 is probably only slightly misfolded because, in our assays, it appears to be functional at the restrictive temperature when overproduced or when degradation is inhibited. Accordingly, the proteasome and Pib1 also play a role in regulating wild-type Sec3. In conclusion, our data corroborate previous findings showing that missense proteins are targeted for degradation and reveal a so far unreported chaperone-assisted degradation pathway (Fig. 9).

## *Experimental procedures*

### *Yeast strains and techniques*

The fission yeast strains used in this study (supplemental Table S1) are derivatives of the wild-type heterothallic strains *972h*$^-$ and *975h*$^+$. Some strains were purchased from Bioneer (72). Standard genetic methods and media were used, and *S. pombe* transformations were performed using lithium acetate (73). The PCR mutagenesis and marker switch were performed as described previously (74, 75).

### *Plasmids*

The *pib1*$^+$ (SPBC36B7.05c) cDNAs were purchased from GeneArt in the pENTR221 vector and transferred to the pDUAL vector (76) for expression in *S. pombe* using the Gateway cloning system (Invitrogen).

### *Growth assays*

Growth assays on solid medium were performed essentially as described previously (77). Briefly, the *S. pombe* strains to be assayed were grown to an $A_{600\,nm}$ of 0.4–0.8. The cells were then diluted in medium to an $A_{600\,nm}$ of exactly 0.40. Serial 5-fold dilutions of this culture were prepared before 5 $\mu$l of each dilution was spotted onto solid medium plates (Edinburgh minimal medium 2 (EMM2) (Biomol) for plasmid selection, otherwise yeast extract with supplements (YES; 30 g/l glucose, 5 g/l yeast extract, 225 mg/l adenine, 225 mg/l leucine, 225 mg/l uracil)) and incubated at the indicated temperature until colonies formed.

### *Electrophoresis and blotting*

Proteins were separated on 7 cm × 8 cm 12% acrylamide gels and subsequently transferred to 0.2-$\mu$m pore size nitrocellulose membranes. Membranes were blocked in PBS (133 mM NaCl, 2.7 mM KCl, 6.5 mM $Na_2HPO_4$, and 1.5 mM $KH_2PO_4$ (pH 7.4)) containing 5% fat-free milk powder and 0.01% Tween 20. Membranes were then probed with the indicated antibodies overnight. The antisera, used in Western blots diluted 1:1000, were as follows: anti-GFP (clone 3H9, Chromotek), anti-V5 (clone SV5, Serotec), anti-$His_6$ (catalog no. 34660, Qiagen), anti-Hsp70 (clone 5A5, Abcam), and anti-$\alpha$-tubulin (clone TAT1, Abcam). Secondary antibodies were purchased HRP-conjugated from Dako Cytomation.

### *Cell imaging and fluorescence microscopy*

Cell septation was monitored by staining with calcofluor white (Sigma) as described previously (11). Endocytosis was monitored by following FM4-64 uptake over time as described previously (11). Cells were imaged on 2% agarose pads using an Olympus IX71 wide-field inverted epifluorescence microscope. An Olympus ×63 numerical aperture 1.4 oil immersion objective was used, and images were captured with a Coolsnap-HQ2 charge-coupled device camera. Counts, measurements, and image presentations were made using Metamorph (Molecular Devices) and downloaded to Microsoft Excel or GraphPad for analyses.

### *Transmission electron microscopy*

For electron microscopy studies, $10^6$ cells in YES were fixed in 2% (v/v) glutaraldehyde and 2% (v/v) formaldehyde in PBS, washed with buffer, and sedimented for 10 min at 17,000 × *g*. The cells were then post-fixed using 2% potassium permanganate, washed with water, dehydrated through a graded ethanol series (50% to 100% ethanol), and embedded in Durcupan resin (Sigma). Ultrathin sections (70 nm) were collected on pioloform-coated EM copper grids (Agar Scientific) and contrasted using lead citrate. Sections were analyzed using a JEOL JEM 1400 transmission electron microscope operated at 120 kV, and images were obtained at a nominal magnification of 12,000 with a digital camera (ES1000 W, Gatan).

For estimating the fractional volume of vesicles inside the cytoplasm, sections were sampled systematic uniform random in three independent experiments ($n > 202$ cells in total) (78). The sampled micrographs were then overlaid with a randomly placed square grid lattice in Metamorph (Molecular Devices) and the areas (A) of interest estimated by point counting (point spacing 50 pixels and 350 pixels for vesicles and cytoplasm, respectively). The mean volume density of vesicles in the cytoplasm is then given by $\Sigma A_{vesicle}/\Sigma A_{cytoplasm}$. Vesicles were identified by the presence of a single membrane, a round to oval profile shape, and a dark and homogenously contrasted matrix. Results were downloaded to GraphPad for analyses.

### *Protein degradation assays*

The degradation of the V5-tagged Sec3 and Sec3-913 proteins was followed in cycloheximide-treated cultures by electrophoresis and blotting as described previously (79). Protein was extracted in TCA using glass beads. Briefly, harvested cells were resuspended in 20% TCA. Then glass beads were added, and the samples were subjected to three rounds of 15 s in a FastPrep machine (Thermo). The glass beads and unbroken cells were removed by centrifugation (1000 × *g*, 5 min.). The supernatant was further centrifuged (10,000 × *g*, 5 min), and the resulting pellet was extensively washed with ice-cold acetone. Finally, the pellet was resuspended in SDS-PAGE loading buffer (50 mM Tris/HCl (pH 6.8), 2% SDS, 0.1% $\beta$-mercaptoethanol, 10% glycerol, and 0.2 mg/ml bromphenol blue). Antibodies to $\alpha$-tubulin (Abcam) were used as the loading control. Quantification was performed by densitometry using the UnScan-It Gel v6.1 software (Silk Scientific Corp.). Bortezomib was purchased from LC Laboratories.

### *Ubiquitylation of Sec3-913*

The ubiquitylation of Sec3-913-V5 was determined by precipitating $His_6$-ubiquitin under denaturing conditions (in 8 M urea), followed by electrophoresis and blotting for the V5 tag on Sec3-913 as described previously (80).

*Author contributions*—C. K., A. K., A. B. A., A. M. L., S. M. S., and I. J. conducted the experiments. I. J. and R. H. P. conceived the project. C. K., I. J., and R. H. P. designed the experiments, analyzed the data, and wrote the paper.

*Acknowledgments—We thank Christian Hacker (Bioimaging Centre, University of Exeter) for technical assistance with the EM experiments. We also thank Dr. Olaf Nielsen, Dr. Colin Gordon, Dr. Klavs B. Hendil, Dr. Michael Seeger, and Dr. Franziska Kriegenburg for helpful discussions and comments on the manuscript.*

**References**

1. Martín-Cuadrado, A. B., Dueñas, E., Sipiczki, M., Vázquez de Aldana, C. R., and del Rey, F. (2003) The endo-$\beta$-1,3-glucanase eng1p is required for dissolution of the primary septum during cell separation in *Schizosaccharomyces pombe*. *J. Cell Sci.* **116,** 1689–1698
2. Cai, H., Reinisch, K., and Ferro-Novick, S. (2007) Coats, tethers, Rabs, and SNAREs work together to mediate the intracellular destination of a transport vesicle. *Dev. Cell* **12,** 671–682
3. He, B., and Guo, W. (2009) The exocyst complex in polarized exocytosis. *Curr. Opin. Cell Biol.* **21,** 537–542
4. Martin-Urdiroz, M., Deeks, M. J., Horton, C. G., Dawe, H. R., and Jourdain, I. (2016) The exocyst complex in health and disease. *Front. Cell Dev. Biol.* **4,** 24
5. Heider, M. R., Gu, M., Duffy, C. M., Mirza, A. M., Marcotte, L. L., Walls, A. C., Farrall, N., Hakhverdyan, Z., Field, M. C., Rout, M. P., Frost, A., and Munson, M. (2016) Subunit connectivity, assembly determinants and architecture of the yeast exocyst complex. *Nat. Struct. Mol. Biol.* **23,** 59–66
6. Boyd, C., Hughes, T., Pypaert, M., and Novick, P. (2004) Vesicles carry most exocyst subunits to exocytic sites marked by the remaining two subunits, Sec3p and Exo70p. *J. Cell Biol.* **167,** 889–901
7. He, B., Xi, F., Zhang, X., Zhang, J., and Guo, W. (2007) Exo70 interacts with phospholipids and mediates the targeting of the exocyst to the plasma membrane. *EMBO J.* **26,** 4053–4065
8. Liu, J., Zuo, X., Yue, P., and Guo, W. (2007) Phosphatidylinositol 4,5-bisphosphate mediates the targeting of the exocyst to the plasma membrane for exocytosis in mammalian cells. *Mol. Biol. Cell* **18,** 4483–4492
9. Pleskot, R., Cwiklik, L., Jungwirth, P., Žárský, V., and Potocký, M. (2015) Membrane targeting of the yeast exocyst complex. *Biochim. Biophys. Acta* **1848,** 1481–1489
10. Jin, Y., Sultana, A., Gandhi, P., Franklin, E., Hamamoto, S., Khan, A. R., Munson, M., Schekman, R., and Weisman, L. S. (2011) Myosin V trans-

ports secretory vesicles via a Rab GTPase cascade and interaction with the exocyst complex. *Dev. Cell* **21,** 1156–1170
11. Jourdain, I., Dooley, H. C., and Toda, T. (2012) Fission yeast sec3 bridges the exocyst complex to the actin cytoskeleton. *Traffic* **13,** 1481–1495
12. Wang, H., Tang, X., Liu, J., Trautmann, S., Balasundaram, D., McCollum, D., and Balasubramanian, M. K. (2002) The multiprotein exocyst complex is essential for cell separation in *Schizosaccharomyces pombe*. *Mol. Biol. Cell* **13,** 515–529
13. Martín-Cuadrado, A. B., Morrell, J. L., Konomi, M., An, H., Petit, C., Osumi, M., Balasubramanian, M., Gould, K. L., Del Rey, F., de Aldana, C. R. (2005) Role of septins and the exocyst complex in the function of hydrolytic enzymes responsible for fission yeast cell separation. *Mol. Biol. Cell* **16,** 4867–4881
14. Bendezú, F. O., Vincenzetti, V., and Martin, S. G. (2012) Fission yeast Sec3 and Exo70 are transported on actin cables and localize the exocyst complex to cell poles. *PLoS ONE* **7,** e40248
15. Wu, H., Rossi, G., and Brennwald, P. (2008) The ghost in the machine: small GTPases as spatial regulators of exocytosis. *Trends Cell Biol.* **18,** 397–404
16. Wu, B., and Guo, W. (2015) The exocyst at a glance. *J. Cell Sci.* **128,** 2957–2964
17. Hartl, F. U., Bracher, A., and Hayer-Hartl, M. (2011) Molecular chaperones in protein folding and proteostasis. *Nature* **475,** 324–332
18. Kriegenburg, F., Ellgaard, L., and Hartmann-Petersen, R. (2012) Molecular chaperones in targeting misfolded proteins for ubiquitin-dependent degradation. *FEBS J.* **279,** 532–542
19. Le Goff, X., Chesnel, F., Delalande, O., Couturier, A., Dréano, S., Le Goff, C., Vigneau, C., and Arlot-Bonnemains, Y. (2016) Aggregation dynamics and identification of aggregation-prone mutants of the von Hippel-Lindau tumor suppressor protein. *J. Cell Sci.* **129,** 2638–2650
20. Gardner, R. G., Nelson, Z. W., and Gottschling, D. E. (2005) Degradation-mediated protein quality control in the nucleus. *Cell* **120,** 803–815
21. Kriegenburg, F., Jakopec, V., Poulsen, E. G., Nielsen, S. V., Roguev, A., Krogan, N., Gordon, C., Fleig, U., and Hartmann-Petersen, R. (2014) A chaperone-assisted degradation pathway targets kinetochore proteins to ensure genome stability. *PLoS Genet.* **10,** e1004140
22. Meacham, G. C., Patterson, C., Zhang, W., Younger, J. M., and Cyr, D. M. (2001) The Hsc70 co-chaperone CHIP targets immature CFTR for proteasomal degradation. *Nat. Cell Biol.* **3,** 100–105
23. Ahner, A., Nakatsukasa, K., Zhang, H., Frizzell, R. A., and Brodsky, J. L. (2007) Small heat-shock proteins select δF508-CFTR for endoplasmic reticulum-associated degradation. *Mol. Biol. Cell* **18,** 806–814
24. Amm, I., Sommer, T., and Wolf, D. H. (2014) Protein quality control and elimination of protein waste: the role of the ubiquitin-proteasome system. *Biochim. Biophys. Acta* **1843,** 182–196
25. Christianson, J. C., and Ye, Y. (2014) Cleaning up in the endoplasmic reticulum: ubiquitin in charge. *Nat. Struct. Mol. Biol.* **21,** 325–335
26. Guerriero, C. J., Weiberth, K. F., and Brodsky, J. L. (2013) Hsp70 targets a cytoplasmic quality control substrate to the San1p ubiquitin ligase. *J. Biol. Chem.* **288,** 18506–18520
27. Nielsen, S. V., Poulsen, E. G., Rebula, C. A., and Hartmann-Petersen, R. (2014) Protein quality control in the nucleus. *Biomolecules* **4,** 646–661
28. Park, S. H., Kukushkin, Y., Gupta, R., Chen, T., Konagai, A., Hipp, M. S., Hayer-Hartl, M., and Hartl, F. U. (2013) PolyQ proteins interfere with nuclear degradation of cytosolic proteins by sequestering the Sis1p chaperone. *Cell* **154,** 134–145
29. Maurer, M. J., Spear, E. D., Yu, A. T., Lee, E. J., Shahzad, S., and Michaelis, S. (2016) Degradation signals for ubiquitin-proteasome dependent cytosolic protein quality control (CytoQC) in yeast. *G3* **6,** 1853–1866
30. Fang, N. N., Chan, G. T., Zhu, M., Comyn, S. A., Persaud, A., Deshaies, R. J., Rotin, D., Gsponer, J., and Mayor, T. (2014) Rsp5/Nedd4 is the main ubiquitin ligase that targets cytosolic misfolded proteins following heat stress. *Nat. Cell Biol.* **16,** 1227–1237
31. Geffen, Y., Appleboim, A., Gardner, R. G., Friedman, N., Sadeh, R., and Ravid, T. (2016) Mapping the landscape of a eukaryotic degronome. *Mol. Cell* **63,** 1055–1065
32. Gordon, C., McGurk, G., Dillon, P., Rosen, C., and Hastie, N. D. (1993) Defective mitosis due to a mutation in the gene for a fission yeast 26S protease subunit. *Nature* **366,** 355–357
33. Jäntti, J., Lahdenranta, J., Olkkonen, V. M., Söderlund, H., and Keränen, S. (1999) SEM1, a homologue of the split hand/split foot malformation candidate gene Dss1, regulates exocytosis and pseudohyphal differentiation in yeast. *Proc. Natl. Acad. Sci. U.S.A.* **96,** 909–914
34. Paraskevopoulos, K., Kriegenburg, F., Tatham, M. H., Rösner, H. I., Medina, B., Larsen, I. B., Brandstrup, R., Hardwick, K. G., Hay, R. T., Kragelund, B. B., Hartmann-Petersen, R., and Gordon, C. (2014) Dss1 is a 26S proteasome ubiquitin receptor. *Mol. Cell* **56,** 453–461
35. Kragelund, B. B., Schenstrøm, S. M., Rebula, C. A., Panse, V. G., and Hartmann-Petersen, R. (2016) DSS1/Sem1, a multifunctional and intrinsically disordered protein. *Trends Biochem. Sci.* **41,** 446–459
36. Gachet, Y., and Hyams, J. S. (2005) Endocytosis in fission yeast is spatially associated with the actin cytoskeleton during polarised cell growth and cytokinesis. *J. Cell Sci.* **118,** 4231–4242
37. Rosenbaum, J. C., Fredrickson, E. K., Oeser, M. L., Garrett-Engele, C. M., Locke, M. N., Richardson, L. A., Nelson, Z. W., Hetrick, E. D., Milac, T. I., Gottschling, D. E., and Gardner, R. G. (2011) Disorder targets misorder in nuclear quality control degradation: a disordered ubiquitin ligase directly recognizes its misfolded substrates. *Mol. Cell* **41,** 93–106
38. Finley, D. (2011) Misfolded proteins driven to destruction by Hul5. *Nat. Cell Biol.* **13,** 1290–1292
39. Bays, N. W., Gardner, R. G., Seelig, L. P., Joazeiro, C. A., and Hampton, R. Y. (2001) Hrd1p/Der3p is a membrane-anchored ubiquitin ligase required for ER-associated degradation. *Nat. Cell Biol.* **3,** 24–29
40. Mathiassen, S. G., Larsen, I. B., Poulsen, E. G., Madsen, C. T., Papaleo, E., Lindorff-Larsen, K., Kragelund, B. B., Nielsen, M. L., Kriegenburg, F., and Hartmann-Petersen, R. (2015) A two-step protein quality control pathway for a misfolded DJ-1 variant in fission yeast. *J. Biol. Chem.* **290,** 21141–21153
41. Fang, N. N., Ng, A. H., Measday, V., and Mayor, T. (2011) Hul5 HECT ubiquitin ligase plays a major role in the ubiquitylation and turnover of cytosolic misfolded proteins. *Nat. Cell Biol.* **13,** 1344–1352
42. Fang, N. N., Zhu, M., Rose, A., Wu, K. P., and Mayor, T. (2016) Deubiquitinase activity is required for the proteasomal degradation of misfolded cytosolic proteins upon heat-stress. *Nat. Commun.* **7,** 12907
43. Tamai, K. K., and Shimoda, C. (2002) The novel HECT-type ubiquitin-protein ligase Pub2p shares partially overlapping function with Pub1p in *Schizosaccharomyces pombe*. *J. Cell Sci.* **115,** 1847–1857
44. Liu, X. M., Sun, L. L., Hu, W., Ding, Y. H., Dong, M. Q., and Du, L. L. (2015) ESCRTs cooperate with a selective autophagy receptor to mediate vacuolar targeting of soluble cargos. *Mol. Cell* **59,** 1035–1042
45. Burd, C. G., and Emr, S. D. (1998) Phosphatidylinositol(3)-phosphate signaling mediated by specific binding to RING FYVE domains. *Mol. Cell* **2,** 157–162
46. Shin, M. E., Ogburn, K. D., Varban, O. A., Gilbert, P. M., and Burd, C. G. (2001) FYVE domain targets Pib1p ubiquitin ligase to endosome and vacuolar membranes. *J. Biol. Chem.* **276,** 41388–41393
47. Yamamoto, A., Mizukami, Y., and Sakurai, H. (2005) Identification of a novel class of target genes and a novel type of binding sequence of heat shock transcription factor in *Saccharomyces cerevisiae*. *J. Biol. Chem.* **280,** 11911–11919
48. Crosas, B., Hanna, J., Kirkpatrick, D. S., Zhang, D. P., Tone, Y., Hathaway, N. A., Buecker, C., Leggett, D. S., Schmidt, M., King, R. W., Gygi, S. P., and Finley, D. (2006) Ubiquitin chains are remodeled at the proteasome by opposing ubiquitin ligase and deubiquitinating activities. *Cell* **127,** 1401–1413
49. Lee, B. H., Lee, M. J., Park, S., Oh, D. C., Elsasser, S., Chen, P. C., Gartner, C., Dimova, N., Hanna, J., Gygi, S. P., Wilson, S. M., King, R. W., and Finley, D. (2010) Enhancement of proteasome activity by a small-molecule inhibitor of USP14. *Nature* **467,** 179–184
50. Mazumdar, T., Gorgun, F. M., Sha, Y., Tyryshkin, A., Zeng, S., Hartmann-Petersen, R., Jørgensen, J. P., Hendil, K. B., and Eissa, N. T. (2010) Regulation of NF-κB activity and inducible nitric oxide synthase by regulatory particle non-ATPase subunit 13 (Rpn13). *Proc. Natl. Acad. Sci. U.S.A.* **107,** 13854–13859

51. Mao, P., and Smerdon, M. J. (2010) Yeast deubiquitinase Ubp3 interacts with the 26S proteasome to facilitate Rad4 degradation. *J. Biol. Chem.* **285,** 37542–37550
52. Kono, K., Saeki, Y., Yoshida, S., Tanaka, K., and Pellman, D. (2012) Proteasomal degradation resolves competition between cell polarization and cellular wound healing. *Cell* **150,** 151–164
53. Capecchi, M. R., Capecchi, N. E., Hughes, S. H., and Wahl, G. M. (1974) Selective degradation of abnormal proteins in mammalian tissue culture cells. *Proc. Natl. Acad. Sci. U.S.A.* **71,** 4732–4736
54. Drummond, D. A. (2009) Protein evolution: innovative chaps. *Curr. Biol.* **19,** R740–R742
55. Van Dyk, T. K., Gatenby, A. A., and LaRossa, R. A. (1989) Demonstration by genetic suppression of interaction of GroE products with many proteins. *Nature* **342,** 451–453
56. Queitsch, C., Sangster, T. A., and Lindquist, S. (2002) Hsp90 as a capacitor of phenotypic variation. *Nature* **417,** 618–624
57. Sangster, T. A., Salathia, N., Undurraga, S., Milo, R., Schellenberg, K., Lindquist, S., and Queitsch, C. (2008) HSP90 affects the expression of genetic variation and developmental stability in quantitative traits. *Proc. Natl. Acad. Sci. U.S.A.* **105,** 2963–2968
58. Arndt, V., Rogon, C., and Höhfeld, J. (2007) To be, or not to be: molecular chaperones in protein degradation. *Cell Mol. Life Sci.* **64,** 2525–2541
59. Arlow, T., Scott, K., Wagenseller, A., and Gammie, A. (2013) Proteasome inhibition rescues clinically significant unstable variants of the mismatch repair protein Msh2. *Proc. Natl. Acad. Sci. U.S.A.* **110,** 246–251
60. Nielsen, S. V., Stein, A., Dinitzen, A. B., Papaleo, E., Tatham, M. H., Poulsen, E. G., Kassem, M. M., Rasmussen, L. J., Lindorff-Larsen, K., and Hartmann-Petersen, R. (2017) Predicting the impact of Lynch syndrome-causing missense mutations from structural calculations. *PLoS Genet.* **13,** e1006739
61. Amm, I., and Wolf, D. H. (2016) Molecular mass as a determinant for nuclear San1-dependent targeting of misfolded cytosolic proteins to proteasomal degradation. *FEBS Lett.* **590,** 1765–1775
62. Bengtson, M. H., and Joazeiro, C. A. (2010) Role of a ribosome-associated E3 ubiquitin ligase in protein quality control. *Nature* **467,** 470–473
63. Brandman, O., Stewart-Ornstein, J., Wong, D., Larson, A., Williams, C. C., Li, G. W., Zhou, S., King, D., Shen, P. S., Weibezahn, J., Dunn, J. G., Rouskin, S., Inada, T., Frost, A., and Weissman, J. S. (2012) A ribosome-bound quality control complex triggers degradation of nascent peptides and signals translation stress. *Cell* **151,** 1042–1054
64. Duttler, S., Pechmann, S., and Frydman, J. (2013) Principles of cotranslational ubiquitination and quality control at the ribosome. *Mol. Cell* **50,** 379–393
65. Theodoraki, M. A., Nillegoda, N. B., Saini, J., and Caplan, A. J. (2012) A network of ubiquitin ligases is important for the dynamics of misfolded protein aggregates in yeast. *J. Biol. Chem.* **287,** 23911–23922
66. Fang, Y., Jaiseng, W., Ma, Y., Hu, L., Yamazaki, S., Zhang, X., Hayafuji, T., Shi, L., and Kuno, T. (2014) E3 ubiquitin ligase Pub1 is implicated in endocytosis of a GPI-anchored protein Ecm33 in fission yeast. *PLoS ONE* **9,** e85238
67. Huibregtse, J. M., Yang, J. C., and Beaudenon, S. L. (1997) The large subunit of RNA polymerase II is a substrate of the Rsp5 ubiquitin-protein ligase. *Proc. Natl. Acad. Sci. U.S.A.* **94,** 3656–3661
68. Dunn, R., and Hicke, L. (2001) Domains of the Rsp5 ubiquitin-protein ligase required for receptor-mediated and fluid-phase endocytosis. *Mol. Biol. Cell* **12,** 421–435
69. Shcherbik, N., and Pestov, D. G. (2011) The ubiquitin ligase Rsp5 is required for ribosome stability in *Saccharomyces cerevisiae*. *RNA* **17,** 1422–1428
70. Nishino, K., Kushima, M., Matsuo, Y., Matsuo, Y., and Kawamukai, M. (2015) Cell lysis in *S. pombe* ura4 mutants is suppressed by loss of functional Pub1, which regulates the uracil transporter Fur4. *PLoS ONE* **10,** e0141796
71. Nakashima, A., Kamada, S., Tamanoi, F., and Kikkawa, U. (2014) Fission yeast arrestin-related trafficking adaptor, Arn1/Any1, is ubiquitinated by Pub1 E3 ligase and regulates endocytosis of Cat1 amino acid transporter. *Biol. Open* **3,** 542–552
72. Kim, D. U., Hayles, J., Kim, D., Wood, V., Park, H. O., Won, M., Yoo, H. S., Duhig, T., Nam, M., Palmer, G., Han, S., Jeffery, L., Baek, S. T., Lee, H., Shim, Y. S., *et al.* (2010) Analysis of a genome-wide set of gene deletions in the fission yeast *Schizosaccharomyces pombe*. *Nat. Biotechnol.* **28,** 617–623
73. Moreno, S., Klar, A., and Nurse, P. (1991) Molecular genetic analysis of fission yeast *Schizosaccharomyces pombe*. *Methods Enzymol.* **194,** 795–823
74. Bähler, J., Wu, J. Q., Longtine, M. S., Shah, N. G., McKenzie, A., 3rd, Steever, A. B., Wach, A., Philippsen, P., and Pringle, J. R. (1998) Heterologous modules for efficient and versatile PCR-based gene targeting in *Schizosaccharomyces pombe*. *Yeast* **14,** 943–951
75. Sato, M., Dhut, S., and Toda, T. (2005) New drug-resistant cassettes for gene disruption and epitope tagging in *Schizosaccharomyces pombe*. *Yeast* **22,** 583–591
76. Matsuyama, A., Shirai, A., Yashiroda, Y., Kamata, A., Horinouchi, S., and Yoshida, M. (2004) pDUAL, a multipurpose, multicopy vector capable of chromosomal integration in fission yeast. *Yeast* **21,** 1289–1305
77. Andersen, K. M., Jensen, C., Kriegenburg, F., Lauridsen, A. M., Gordon, C., and Hartmann-Petersen, R. (2011) Txl1 and Txc1 are co-factors of the 26S proteasome in fission yeast. *Antioxid. Redox. Signal* **14,** 1601–1608
78. Lucocq, J. M., and Hacker, C. (2013) Cutting a fine figure: on the use of thin sections in electron microscopy to quantify autophagy. *Autophagy* **9,** 1443–1448
79. Hartmann-Petersen, R., Wallace, M., Hofmann, K., Koch, G., Johnsen, A. H., Hendil, K. B., and Gordon, C. (2004) The Ubx2 and Ubx3 cofactors direct Cdc48 activity to proteolytic and nonproteolytic ubiquitin-dependent processes. *Curr. Biol.* **14,** 824–828
80. Penney, M., Samejima, I., Wilkinson, C. R., McInerny, C. J., Mathiassen, S. G., Wallace, M., Toda, T., Hartmann-Petersen, R., and Gordon, C. (2012) Fission yeast 26S proteasome mutants are multi-drug resistant because of stabilization of the Pap1 transcription factor. *PLoS ONE* **7,** e50796